Importance of the α_s-plot Method in the Characterization of Nanoporous Materials

Jhonny Villarroel-Rocha, Deicy Barrera, Andrés A. García Blanco, Ma. Eugenia Roca Jalil and Karim Sapag

Reprinted from

Adsorption Science & Technology

2013 Volume 31 Number 2+3

Multi-Science Publishing Co. Ltd.
5 Wates Way, Brentwood, Essex CM15 9TB, United Kingdom

Importance of the α_s-plot Method in the Characterization of Nanoporous Materials†

Jhonny Villarroel-Rocha, Deicy Barrera, Andrés A. García Blanco, Ma. Eugenia Roca Jalil and Karim Sapag* *Laboratorio de Sólidos Porosos, INFAP, Universidad Nacional de San Luis-CONICET, Chacabuco 917, 5700 San Luis, Argentina.*

ABSTRACT: In this work, an exhaustive study of the calculation of micropore and mesopore volumes with α_s-plot method as proposed by Professor Sing is carried out. The method is critically compared with other similar methods such as the Dubinin–Radushkevich, t-plot and those based on density functional theory (DFT). For comparison purposes, several nanoporous materials with different chemical properties were selected. The analysis was segregated into three categories: (i) microporous materials, in which the analyzed samples are activated carbons (ACs) with different pore-size distributions, a single-walled carbon nanotube (SWNT) and a zeolite (MS5A); (ii) mesoporous materials, including ordered mesoporous carbons (CMK-3) and ordered mesoporous siliceous materials (MCM-41 and SBA-15); and (iii) micro-mesoporous materials, in which pillared clays (PILCs) obtained with different metals (Al, Si, Fe and Zr) were studied. To apply the α_s-plot method, several standard isotherms previously reported by other authors were considered for the analysis of microporous and mesoporous materials. Furthermore, a series of four reference materials for PILCs were synthesized and their high-resolution nitrogen adsorption isotherms were measured and reported. The results obtained by the α_s-plot method are consistent with those obtained by DFT methods. This consistency highlights the importance of the use of this reliable and versatile method, where the correct selection of the standard isotherm is the most critical aspect to be considered.

INTRODUCTION

Nanoporous materials are those materials with pore sizes below 100 nm (Lu and Zhao 2004) and include the microporous (pore sizes below 2 nm) and mesoporous materials (with pore sizes between 2 and 50 nm). Developments made in theoretical and experimental fields related to nanoporous materials have motivated several studies in recent years (Thommes 2010), which have reported the application of these materials in different fields, such as drug delivery (Wang 2009), adsorption of pollutants (Carabineiro *et al*. 2011; Gil *et al*. 2011), heterogeneous catalysis (Corma and García 2002; Oliveira *et al*. 2008; García Blanco *et al*. 2011), gas storage and separation (Guan *et al*. 2008; Kockrick *et al*. 2010; Solar *et al*. 2010) among others.

The behaviour of porous materials in each of these applications strongly depends on their physicochemical properties, a fact that shows the need to develop techniques to assess those properties in the most reliable way. In this sense, it has been found that textural properties such as specific surface area, pore volumes and pore-size distribution are important factors to be considered while designing new materials as well as in their potential applications (Corma and

* Author to whom all correspondence should be addressed. E-mail: sapag@unsl.edu.ar (K. Sapag).

†Published in the Festschrift of the journal dedicated to Professor K.S.W. Sing to celebrate his 65 years of research in the field of adsorption.

García 2002; García Blanco *et al*. 2010; Kockrick *et al*. 2010). Among the various characterization techniques available, gas adsorption has shown to be adequate to determine these properties for microporous and mesoporous materials (Gregg and Sing 1982; Rouquerol *et al*. 1999; Thommes 2010). However, assessing microporosity is not an easy task. As a result, several methods and models have been proposed, with each method presenting different assumptions, physical criteria or application ranges, resulting in underestimation or overestimation of the final results in some cases.

The first adsorption studies (Langmuir 1916; Brunauer *et al*. 1938) were devoted to determine the monolayer capacity for evaluating the specific surface area of porous solids. In 1947 and 1955, Dubinin and colleagues provided evidence that the mechanism of physisorption in very narrow pores (which they termed as micropores) is not the same as in wider pores or on the open surface (Sing 1998). They then derived a semi-empirical expression to evaluate the micropore volume of porous solids (Dubinin 1960). Later, Lippens and de Boer (1965) developed an empirical method based on the use of the adsorbed layer thickness (termed as t) on a non-porous material in order to construct a plot of the amount adsorbed on a determined sample as a function of t by obtaining the denominated t-plot. The isotherm obtained from this non-porous material was termed as standard isotherm and the adsorbed layer thickness, t, can be obtained by the Brunauer–Emmett–Teller (BET) theory (Brunauer *et al*. 1938). For an unknown sample, the selected standard isotherm should present a constant C value (BET equation) similar to that of the analyzed one. It is known that the BET model produces good results when the isotherm is Type II (Sing *et al*. 1985); however, in some cases, important deviations from this model can occur and the application of t-plot method could give erroneous values.

A modification of the t-plot method named α_s-plot was proposed by Sing (1968), who first indicated that the knowledge of the numerical thickness is irrelevant because the aim is only to compare the shape of the isotherm of the material under study with that of the standard isotherm. Sing proposed to replace the monolayer capacity as normalizing factor by the amount adsorbed at a pre-selected relative pressure, i.e. 0.4. Furthermore, with the aim of obtaining reliable results using the α_s-plot method, he proposed to select a standard isotherm obtained from a material free of pores, especially micropores, with chemical properties similar to the material being analyzed (Gregg and Sing 1982; Rouquerol *et al*. 1999). In this way, this method is not related to the BET model, thereby avoiding the deviations observed for the application of t-plot that are noted in some cases.

The above mentioned methodologies are the so-called macroscopic methods for the characterization of porous materials. The advances made in computational methods helped in developing new microscopic methods based on statistical mechanics, which can describe the configuration of the adsorbed phase on a molecular level (Thommes 2010). These methods were improved with successive works made since 1989 (Seaton *et al*. 1989) and nowadays different methodologies are available, such as the density functional theory (DFT) for the characterization of porous materials with specific pore geometry corresponding to a determined adsorbate–adsorbent interaction (Ravikovitch and Neimark 2006). However, to apply these microscopic methods, in most cases, specialized software with specific kernels is necessary to analyze the experimental adsorption–desorption isotherms.

In this work, a critical study of the calculation of micropore and mesopore volumes by α_s-plot method was carried out and compared with the Dubinin–Radushkevich (DR), t-plot and DFT methods. For this purpose, several nanoporous materials with different chemical properties were selected. Among the samples chosen, activated carbons (ACs) with different pore-size distributions, a single-walled carbon nanotube (SWNT), a zeolite (MS5A), mesoporous carbons

(CMK-3), ordered mesoporous siliceous materials (MCM-41 and SBA-15) and pillared clays (PILCs) were analyzed.

MATERIALS AND METHODS

Materials

Microporous materials

The microporous materials used in this work were three different ACs (AC1, AC2 and AC3), a SWNT and a zeolite (MS5A). The ACs were synthesized from different lignocellulosic materials under different activating conditions.

The AC1 sample was obtained from coconut shells by chemical activation (with a 40% wt of zinc chloride), followed by carbon dioxide activation (developing a 28% burn-off). Details of this procedure are described in García Blanco *et al*. (2010). The AC2 sample was obtained from olive cake (a by-product in olive oil manufacture) by chemical activation (with phosphoric acid in a ratio of 0.42 g P/g of raw material). Details of the procedure are described in Solar *et al*. (2010). The AC3 sample was obtained from peach stones by chemical activation (with phosphoric acid). Details of the procedure are described in Soares Maia *et al*. (2010).

SWNT was a commercial sample of carbon nanotubes obtained by the HiPco process. According to the product sheet, the diameter of the nanotubes is approximately 0.8–1.2 nm. The zeolitic material used in this work was a MS5A (SARM 2012; Quantachrome Instruments).

Mesoporous materials

The selected mesoporous materials include two ordered mesoporous silica materials (MCM-41 and SBA-15) and three nanostructured mesoporous carbons materials (CMK-3_A, CMK-3_B and CMK-3_C). The MCM-41 and SBA-15 samples were synthetized according to the non-hydrothermal procedure described in Barrera *et al*. (2011).

Synthesis of the nanostructured carbons (CMK-3) was performed based on some modifications of different conditions (synthesis) reported earlier (Jun *et al*. 2000; Srinivasu *et al*. 2008). This synthesis was carried out using SBA-15 as the template and different amounts of sucrose as the carbon source. Following polymerization, the composite was carbonized under a nitrogen flow (180 cm^3/minute) at 1173 K with a heating rate of 3 K/minute for 6 hours. The nanostructured carbons were recovered by leaching the mesoporous framework in hydrofluoric acid solution (5% wt) at room temperature for 24 hours. The carbons obtained without template were filtered and washed several times with an equimolar mixture of deionized water and ethanol. Finally, the nanostructured carbons were dried overnight at 353 K.

Micro-mesoporous materials

The micro-mesoporous materials studied were pillared interlayered clays (PILCs) synthesized from a natural clay (NC, montmorillonite) using different oligocations.

The silica-pillared clay (Si-PILC) was synthesized based on the procedure described by Han *et al*. (1997) with some modifications. A NC suspension of 1% wt in deionized water was mixed with a SiO_2–Fe_2O_3 oligocation. The mixture was successively washed with hydrochloric acid and

then with deionized water. The solid obtained was filtered before drying.

The iron-pillared clay (Fe-PILC) was synthesized based on the procedure proposed by Yamanaka *et al*. (1984) in which an aqueous solution of the oligocation $[Fe_3(OCOCH_3)_7OH{\cdot}2H_2O]NO_3$ is added to 1% wt suspension of NC in deionized water. The mixture was stirred for 3 hours and the suspension was filtered, washed with deionized water and then dried.

The aluminium-pillared clay (Al-PILC) was obtained following the methodology proposed by Sapag and Mendioroz (2001). The oligocation $[Al^{IV}Al^{VI}_{12}O_4(OH)_{24}(H_2O)_{12}]^{7+}$ is obtained and added to a 3% wt suspension of NC in deionized water. The solid is then separated by decantation, washed with deionized water by dialysis and then dried.

The zirconium-pillared clay (Zr-PILC) was synthesized based on the methodology proposed by Farfan-Torres *et al*. (1991), involving the addition of oligocation solution $[Zr_4(OH)_{14}(H_2O)_{10}]^{2+}$ to a 1% wt suspension of NC in deionized water. The mixture was stirred for 2 hours, filtered, washed with deionized water and then dried.

All the PILC precursors were calcined at 773 K for 1 hour to obtain the Si-PILC, Fe-PILC, Al-PILC and Zr-PILC samples.

Characterization

Nitrogen adsorption–desorption at 77 K

Samples analyzed were characterized by nitrogen (99.999%) adsorption–desorption isotherms at 77 K. These samples were previously degassed for 12 hours up to a residual pressure of 0.5 Pa with different temperatures for the samples analyzed (523 K for the carbonaceous microporous materials, 673 K for the MS5A sample and 473 K for the other materials). These measurements were carried out using Autosorb 1MP and iQ (Quantachrome Instruments) and ASAP 2000 (Micromeritics Instrument Corporation).

Methods

The BET method (Brunauer *et al*. 1938) was used to estimate the specific surface area (S_{BET}) of the samples, in which the conditions of linearity and considerations regarding the method were fulfilled.

The DR, t-plot, α_s-plot and DFT methods were used to analyze the experimental data obtained from nitrogen adsorption isotherms.

DR equation is given by equation (1) as follows:

$$\log(V) = \log\left(V_{\mu P}\right) - \left(\frac{RT}{\beta E_0}\right)^2 \cdot \log^2\left(\frac{p^0}{p}\right) \quad (1)$$

where V corresponds to the volume adsorbed; $V_{\mu P}$ is the micropore volume expressed as liquid volume, assuming that the density of the adsorbed phase is equal to that of the adsorbate in the liquid phase; T is the temperature of the adsorption experiment; β, is the affinity coefficient and E_0 is the characteristic adsorption energy. The applicability range of DR equation is usually between 10^{-5} and 0.2–0.4 of relative pressure, considering that all micropores have been filled in this p/p^0 range (Dubinin 1960).

The t-plot method compares an isotherm of a porous material with a standard isotherm of a

non-porous material (Lippens and de Boer 1965). To apply this method, the experimental isotherm data are used to calculate the adsorbed layer thickness, t, by applying different t equations. By plotting the adsorbed liquid volume versus t, a straight line in the multi-layer region is obtained. The intercept of equation (2) gives the micropore volume, whereas its slope (m_t) is related to the external surface (S_{ext}, in m^2/g). S_{ext} corresponds to the area of those pores that are not micropores.

$$S_{ext} = m_t \times 1000 \tag{2}$$

Table 1 shows the reported t equations for several materials and their respective application ranges.

The α_s-plot is a method similar to the t-plot, but without assuming any adsorbed layer thickness value (Sing 1968). In the former method, the standard isotherm used is a plot of α_s versus p/p^0, in which the α_s values are the amounts adsorbed on a reference material normalized by its amount adsorbed at a relative pressure of 0.4 [$V^{0.4}_{(ref)}$]. The reference material is a non-porous sample, with chemical composition similar to the sample being analyzed. From these data, the α_s-plot is obtained by plotting the adsorbed liquid volume versus α_s, in the manner similar to that described for t-plot. The S_{ext} value (in m^2/g) is obtained by relating the slope of the straight line of the α_s-plot (m_α) to the $V^{0.4}_{(ref)}$ value (in cm^3 STP/g), and $S_{BET(ref)}$ (in m^2/g) for a reference material, as shown in equation (3).

$$S_{ext} = m_\alpha \times \frac{S_{BET(ref)}}{V^{0.4}_{(ref)} \times 0.0015468} \tag{3}$$

In addition, in mesoporous materials, with a well-defined capillary condensation step, a second linear region at high α_s values allows us to obtain information about the mesoporous volume (V_{MP}) of the material being analyzed.

The microscopic methods based on DFT were applied using the software of the equipment, which is described in each case.

RESULTS AND DISCUSSION

Microporous Materials

Figure 1 shows the nitrogen adsorption–desorption isotherms at 77 K for the five microporous materials analyzed. It can be seen that all these materials show high adsorbed amounts at low relative pressures, which is due to the presence of micropores. AC3 and MS5A samples are Type I isotherms, often associated with materials that are basically microporous (Sing *et al.* 1985), while the AC1, AC2 and SWNT samples exhibited hysteresis loops, which indicate the presence of mesopores in these materials.

The isotherms, for the three ACs, show an increasing mesoporosity, which is reflected in the slope of the adsorption branch at relative pressures > 0.1. The SWNT sample showed an abrupt increase at relative pressures higher than 0.8, which is due to the presence of larger mesopores.

Table 2 shows the textural properties of microporous materials based on the nitrogen adsorption isotherms. The micropore volumes were calculated by different methods to compare

TABLE 1. t Equations for Different Nanoporous Materials

Equation	Expression (t in nm)	Application range of p/p^0	Samples	References
Halsey (H) or Frenkel–Halsey–Hill (FHH)	$t = 0.354 \cdot \left[\frac{-5}{\ln\left(\frac{p}{p^0}\right)}\right]^{\frac{1}{3}}$ (1)	0.1–0.75	Silica, alumina and other oxides	[a], [b]
Harkins–Jura (HJ) or de Boer (dB)	$t = 0.1 \cdot \left[\frac{13.99}{0.034 - \log\left(\frac{p}{p^0}\right)}\right]^{\frac{1}{2}}$ (2)	0.1–0.75	Oxides, hydroxides, natural and pillared clays, and zeolitic materials	[c], [b]
Broekhoff–de Boer (BdB)	$\log\left(\frac{p}{p^0}\right) = -\frac{0.1611}{t^2} + 0.1682 \cdot \exp\left(-1.137 \cdot t\right)$ (3)	0.3–0.96	Oxide and hydroxide adsorbents	[d]
Harkins–Jura/Kruk–Jaroniec –Sayari (HK–KJS)	$t = 0.1 \cdot \left[\frac{60.65}{0.03071 - \log\left(\frac{p}{p^0}\right)}\right]^{0.3968}$ (4)	0.1–0.95	Ordered mesoporous silica materials such as MCM-41, SBA-15.	[e]
Carbon black (CB)	$t = 0.088 \cdot \left(\frac{p}{p^0}\right)^2 + 0.645 \cdot \left(\frac{p}{p^0}\right) + 0.298$ (5)	0.2–0.5	Carbonaceous materials	[f]

[a] Halsey (1948); [b] de Boer et al. (1966); [c] Harkins and Jura (1944); [d] Broekhoff and de Boer (1967); [e] Kruk et al. (1997b); [f] Magee (1995)

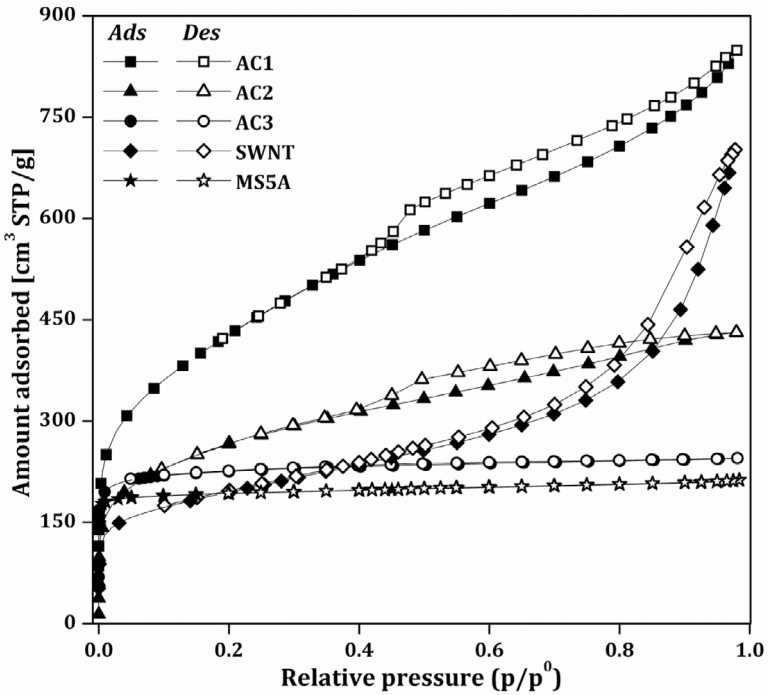

Figure 1. Nitrogen adsorption–desorption isotherms at 77 K for microporous materials.

TABLE 2. Textural Properties of Microporous Materials

Samples	S_{BET} (m^2/g)	$V_{\mu P\text{-}DR}$ (cm^3/g)	t-plot		α_s-plot		$V_{\mu P\text{-}DFT}$ (cm^3/g)
			$V_{\mu P\text{-}t}$ (cm^3/g)	S_{ext} (m^2/g)	$V_{\mu P\text{-}\alpha}$ (cm^3/g)	S_{ext} (m^2/g)	
AC3	890	0.34	0.33	50	0.33	45	0.33
AC2	955	0.35	0.25	410	0.24	440	0.24
AC1	1550	0.54	0.33	890	0.27	995	0.27
SWNT	695	0.28	0.11	445	0.16	320	0.14
MS5A	785	0.29	0.27	55	0.27	70	0.30

differences among them. Micropore volumes obtained by the DR equation [equation (1)] were calculated in a range of relative pressures between 10^{-5} and 10^{-2}. The t equations used in the t-plot method for carbonaceous and zeolitic materials were carbon black (CB) and Harkins–Jura (HJ), respectively (Table 1). The $V_{\mu P\text{-}DFT}$ values, which correspond to the cumulative pore volumes at 2 nm pore sizes, were obtained using the quenched solid state density functional theory (QSDFT) kernel for carbons (Neimark *et al*. 2009) and the non-localized density functional theory (NLDFT) kernel for silicas (Neimark and Ravikovitch 2001) based on the adsorption data for carbonaceous and zeolitic materials, respectively. In the case of α_s-plot method, several standard isotherms for nitrogen adsorption at 77 K are reported for carbonaceous materials. Some of them were obtained

from different non-porous carbons, which could be non-graphitized [e.g. CarbonA (Rodriguez-Reinoso *et al*. 1987), Elftex 120 (Carrott *et al*. 1987), NPCII (Kaneko *et al*. 1992) and Cabot BP 280 (Kruk *et al*. 1997a)] or graphitized [GCB-1 (Nakai *et al*. 2010)]. Considering the requirement for standard isotherms, a non-graphitized CB was selected for ACs. Among the standard isotherms mentioned for this kind of materials, the high-resolution adsorption isotherm for Cabot BP 280 was selected because its data can be extended up to relative pressures significantly lower than the other reference materials; however, taking into account the structure carbon nanotubes, the graphitized CB (GCB-1) was chosen. Regarding the MS5A material, Fransil-I, non-porous hydroxylated silica (Bhambhani *et al*. 1972), was selected as the reference material.

Figure 2 presents various examples of the fits obtained by applying the specified methods for calculating the micropore volumes of a microporous (AC3) and a micro-mesoporous (AC1) carbon.

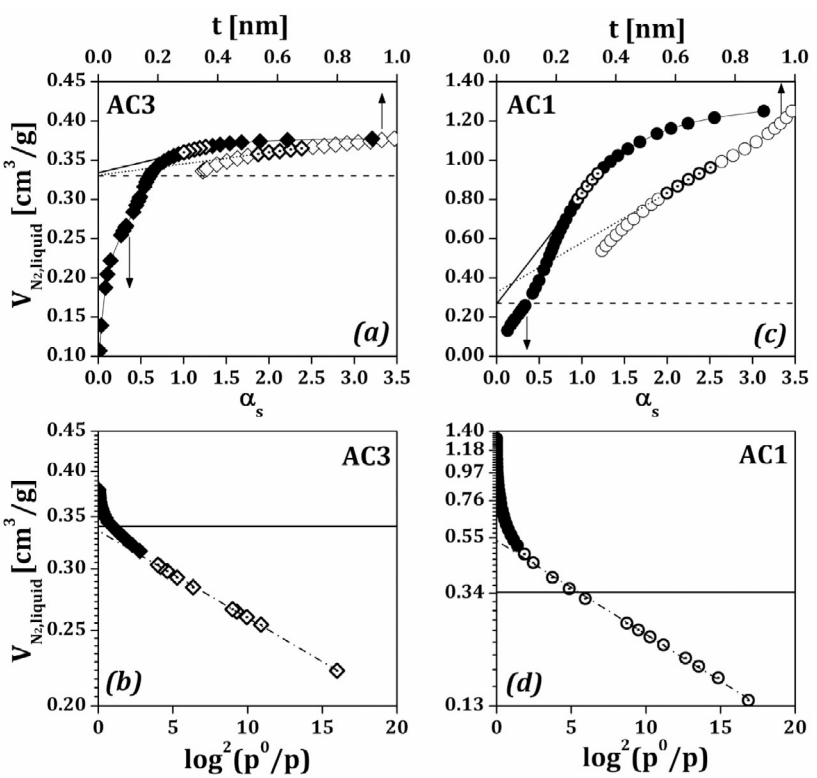

Figure 2. (a and c) t (open symbols) and α_s (filled symbols) plots and (b and d) DR plots with their respective fits for AC3 and AC1 samples. The symbols ⊙ and ◇ are the selected points for the fits. Y axis intercepts correspond to $V_{\mu P\text{-}\alpha}$ (—), $V_{\mu P\text{-}t}$ (···) in (a) and (c); and $V_{\mu P\text{-}DR}$ (-·-·) in (b) and (d). Horizontal dashed line in (a) and (c) represents the $V_{\mu P\text{-}DFT}$ value. The horizontal solid line in (b) and (d) represents the $V_{\mu P\text{-}\alpha}$ value.

Our results of the fit showed that micropore volumes obtained by these methods were basically similar in microporous materials (AC3 and MS5A), as shown in Figures 3(a and b). However, for the other carbonaceous materials (AC1, AC2 and SWNT), the micropore volumes present differences between them, which are related to the high mesoporosity proportion, as shown in

Figures 3(c and d). An overestimation in the $V_{\mu P\text{-}DR}$ value in comparison with those obtained by other methods can be noted in the figure. This overestimation increases with the mesoporosity. Similar results had been reported previously by several authors (Remy and Poncelet 1995; Falabella *et al*. 1998; Brouwer *et al*. 2007). Another interesting note is that small differences between $V_{\mu P\text{-}t}$ and $V_{\mu P\text{-}\alpha}$ could be related to the fact that t-plot method uses an empirical equation for estimating the t values, whereas α_s-plot method uses experimental data. Furthermore, a good agreement between $V_{\mu P\text{-}DFT}$ and $V_{\mu P\text{-}\alpha}$ was found.

Mesoporous Materials

Figure 3 shows the nitrogen adsorption–desorption isotherms at 77 K for carbonaceous [Figure 4(a)] and siliceous [Figure 4(b)] ordered mesoporous materials. All of these materials exhibit Type IV isotherms with hysteresis loops, typical of mesoporous solids. The increase in adsorption at low relative pressures are related to the presence of micropores or can be attributed to a strong adsorbate–adsorbent interaction, as in the case of MCM-41, which does not have any micropores (Silvestre-Albero *et al*. 2009).

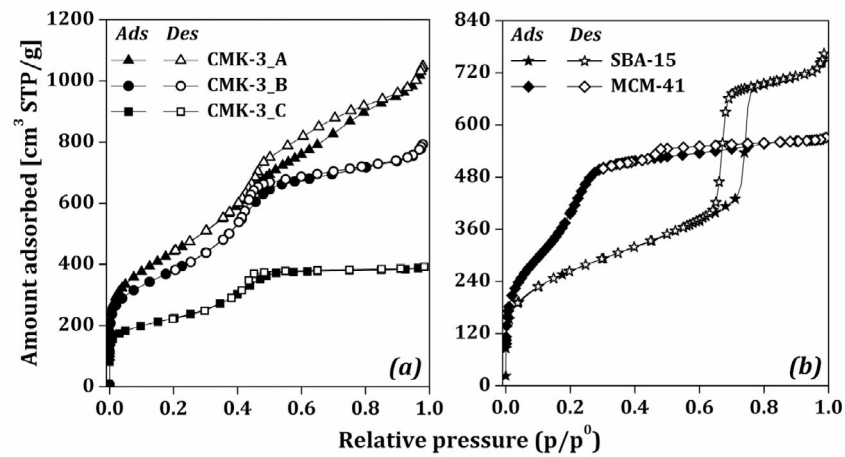

Figure 3. Nitrogen adsorption–desorption isotherms at 77 K for (a) carbonaceous and (b) siliceous ordered mesoporous materials.

Figure 3(a) shows the steps corresponding to the filling of primary mesopores (capillary condensation) at relative pressures > 0.3. The capillary condensation occurs at relative pressures in the range of 0.1–0.35 and 0.65–0.8 for MCM-41 and SBA-15 materials, respectively, due to their mesopore sizes [Figure 3(b)].

Textural properties of mesoporous materials are shown in Table 3. The $V_{\mu P\text{-}DR}$ values were obtained in the same range of relative pressures used for microporous materials. The t equations used in the t-plot method for CMK-3 and siliceous materials were CB and HJ–Kruk–Jaroniec–Sayari (KJS) equations, respectively (Table 1). The $V_{MP\text{-}DFT}$ values are the primary mesopore volumes calculated from their pore-size distributions using the hybrid (slit-cylindrical pore) QSDFT kernel for micro-mesoporous carbons (Gor *et al*. 2012) and the NLDFT kernel for silicas (Neimark and Ravikovitch 2001), for CMK-3 and siliceous mesoporous materials, respectively.

TABLE 3. Textural Properties of Carbonaceous and Siliceous Ordered Mesoporous Materials

Samples	S_{BET} (m^2/g)	$V_{\mu P\text{-}DR}$ (cm^3/g)	t-plot				α_s-plot				DFT	
			$V_{\mu P\text{-}t}$ (cm^3/g)	S_t (m^2/g)	$V_{MP\text{-}t}$ (cm^3/g)	S_{ext} (m^2/g)	$V_{\mu P\text{-}\alpha}$ (cm^3/g)	S_t (m^2/g)	$V_{MP\text{-}\alpha}$ (cm^3/g)	S_{ext} (m^2/g)	$V_{\mu P\text{-}DFT}$ (cm^3/g)	$V_{MP\text{-}DFT}$ (cm^3/g)
CMK-3_A	1585	0.55	0.07	1435	– [a]	– [a]	0.20	1085	– [a]	– [a]	0.23	– [a]
CMK-3_B	1350	0.49	0.09	1170	0.66	415	0.15	970	0.71	230	0.20	0.75
CMK-3_C	795	0.29	0.10	570	0.44	45	0.13	485	0.44	25	0.15	0.41
SBA-15	955	0.32	0.09	560	0.87	100	0.08	770	0.92	100	0.08	0.94
MCM-41	1290	0.41	–0.36	1625	0.71	140	0	1275	0.74	140	0	0.77

[a] Disordered material

Previous reports have shown that CMK-3 presents well-defined graphitic domains within their carbon nanorods (Zhou *et al*. 2003; Ignat *et al*. 2010). Taking this fact into account, the standard isotherm selected for applying the α_s-plot method for ordered mesoporous carbons (CMK-3) was the GCB-1. For ordered mesoporous silica materials, the LiChrospher Si-1000 standard isotherm was selected (Jaroniec *et al*. 1999).

Examples of the fits obtained using these methods for calculating the micropore and primary mesopore volumes for CMK-3_C and MCM-41 are shown in Figure 4.

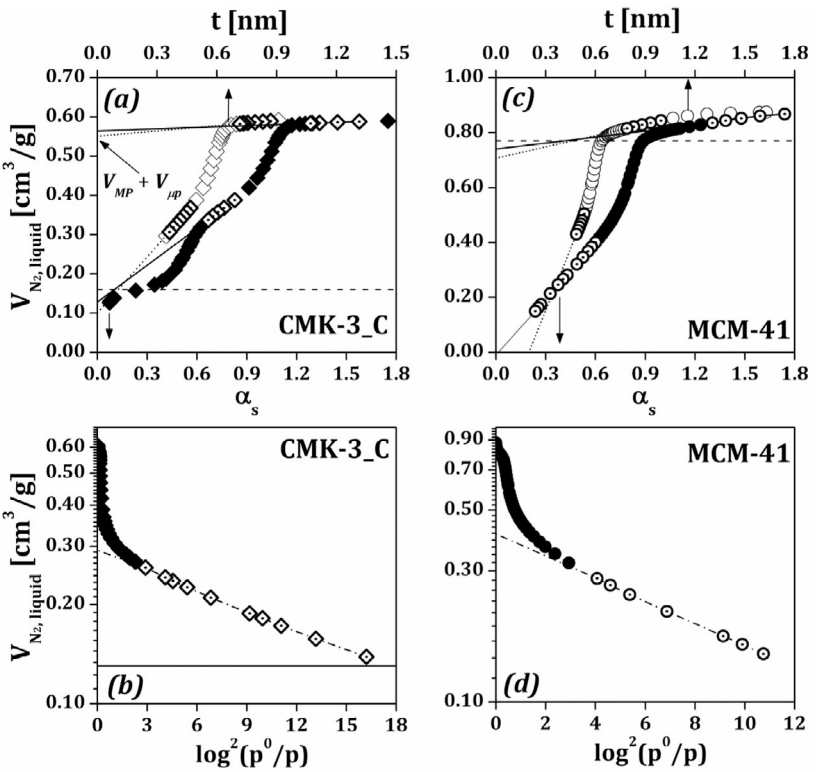

Figure 4. (a and c) t (open symbols) and α_s (filled symbols) plots and (b and d) DR plots with their respective fits for CMK-3_C and MCM-41 samples. The symbols ⊙ and ◇ are the selected points for the fits. Y axis intercepts correspond to $V_{\mu P\text{-}\alpha}$ and $V_{\mu P\text{-}\alpha} + V_{MP\text{-}\alpha}$ (——), $V_{\mu P\text{-}t}$ and $V_{\mu P\text{-}t} + V_{MP\text{-}t}$ (···) in (a) and (c); and $V_{\mu P\text{-}DR}$ (- - -) in (b) and (d). Horizontal dashed line is the $V_{\mu P\text{-}DFT}$ in (a) and $V_{MP\text{-}DFT}$ in (c). The horizontal solid line in (b) represents the $V_{\mu P\text{-}\alpha}$ value.

The results show that the $V_{\mu P\text{-}DR}$ values were highly overestimated compared with the micropore volumes obtained by other methods [Figures 4(a and b)]. This fact can be due to the essentially mesoporous character of CMK-3, SBA-15 and MCM-41 samples. Despite the fact that the MCM-41 is a purely mesoporous material, DR method indicated that it has microporosity [Figure 4(d)]. The $V_{\mu P\text{-}t}$ values obtained for carbonaceous mesoporous materials using the t-plot method were lower than those obtained by the α_s-plot and DFT methods (which presented similar values). These deviations could be related to the fact that the t equation (CB) might not adequately represent these kinds of materials. In the case of the SBA-15 sample, the micropore volumes obtained by t-plot, α_s-plot and DFT methods showed a good agreement. However, the value obtained by the t-plot method for the MCM-41 sample was significantly negative, as observed in

Figure 4(c), due to the limited application range of the t equation (HJ–KJS), which does not allow fitting data at relative pressures below than 0.1.

The micropore volumes obtained using the α_s-plot were consistent with those obtained by the DFT method. However, it is to be noted that the micropore volumes calculated using standard isotherms of non-graphitized CBs do not follow the same tendency as the results reported in Table 3 for $V_{\mu P\text{-}\alpha}$ and $V_{\mu P\text{-}DFT}$. These results reflect the importance of selecting the standard isotherm to calculate the micropore volume. By contrast, the primary mesopore volumes (V_{MP}) obtained by the different methods show a good agreement.

Micro-mesoporous Materials

Figure 5 shows nitrogen adsorption–desorption isotherms at 77 K of different PILCs. These materials present a combination of Type I, at low relative pressures, and Type II isotherms according to the IUPAC classification. The high amount of adsorption at low relative pressures is due to the presence of micropores, which are formed by the pillaring process. The mesoporosity of these materials is evidenced by the presence of hysteresis loops.

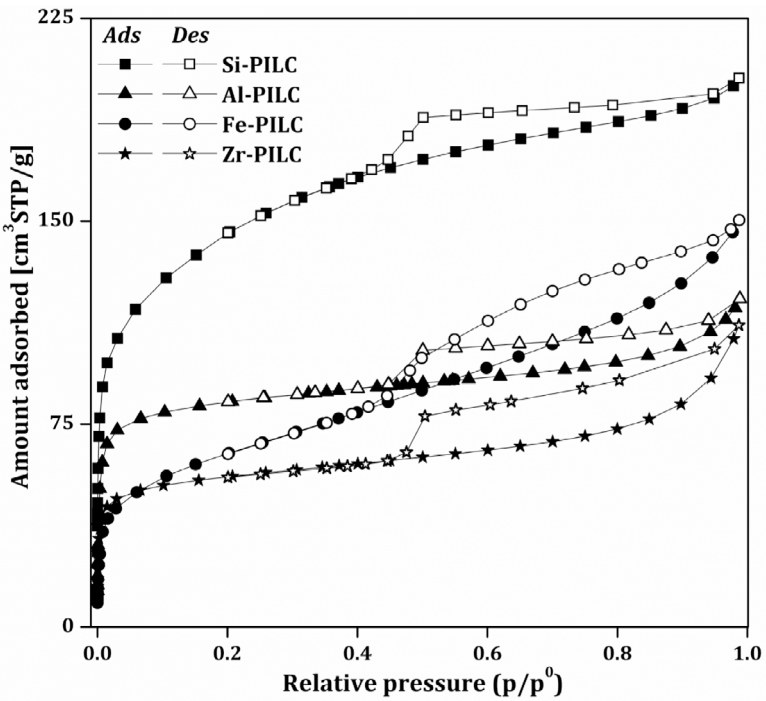

Figure 5. Nitrogen adsorption–desorption isotherms at 77 K for PILC materials.

Standard isotherms of PILCs

Despite the availability of standard isotherms reported for the characterization of different nanoporous materials, standard isotherms for PILCs have not been reported yet. Thus, the α_s-plot method is not frequently used to calculate the micropore volume of PILCs. Very few authors apply

this method using the NC calcined at high temperatures (approximately 1073 K) as the reference material (Gil and Montes 1994; Roca Jalil *et al*. 2013). However, there are no studies regarding the influence of the oxide type formed in the inter-layer during pillaring for standard isotherms.

In this work, nitrogen standard isotherms for PILCs were measured on reference materials obtained by heat treatment of each synthesized PILC (with the different oligocations). Considering the fact that dehydroxylation temperature of the montmorillonite is approximately 873 K and that the fusion of the NC occurs close to 1773 K (de Souza Santos 1989), the calcination temperature was chosen as 1273 K to obtain the reference materials. The samples were calcined with a heating rate of 10 K/minute up to 1273 K, and maintaining this temperature for 1 hour. The reference materials were labelled according to their corresponding oligocation as Si-PILC$_{1273K}$, Al-PILC$_{1273K}$, Fe-PILC$_{1273K}$ and Zr-PILC$_{1273K}$. To perform the nitrogen adsorption isotherm for the reference materials, some authors (Kruk *et al*. 1997a; Nakai *et al*. 2010) have proposed the need for obtaining high-resolution adsorption isotherm data [isotherms from very low relative pressures (approximately 10^{-5}) with enough experimental points (approximately 100)].

The high-resolution nitrogen adsorption isotherms were measured in a manometric equipment (Autosorb-iQ, Quantachrome Instruments), which is equipped with 1000-, 10- and 1-torr transducers that provide high accuracy and high resolution in all the range of relative pressures. These materials were previously degassed at 523 K for 12 hours. Several measurements were performed to guarantee the reliability of the reported data.

Figure 6 shows the high-resolution nitrogen adsorption isotherms at 77 K for Al-PILC$_{1273K}$, Si-PILC$_{1273K}$, Zr-PILC$_{1273K}$ and Fe-PILC$_{1273K}$. For comparative purposes, isotherms of the NC

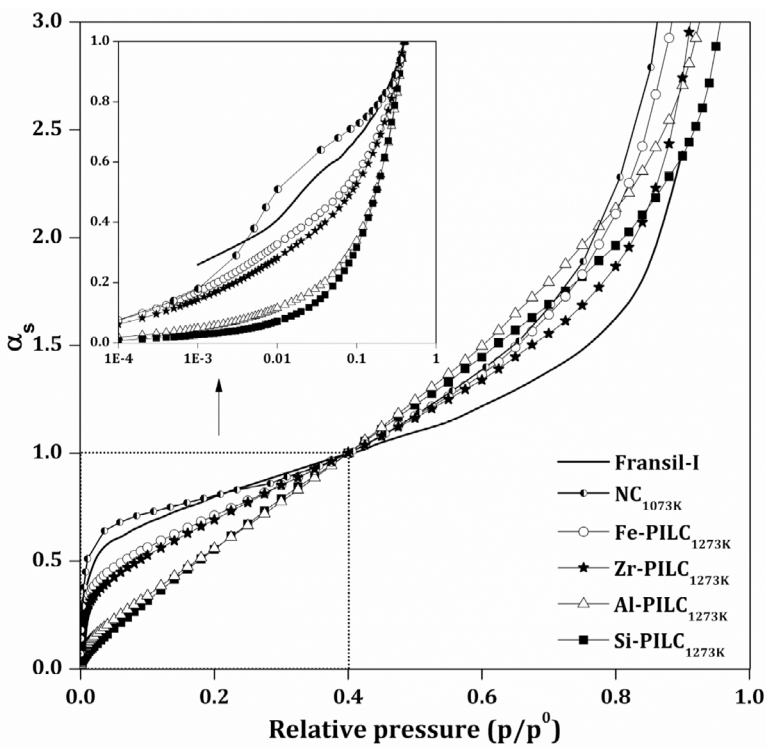

Figure 6. High-resolution nitrogen adsorption isotherms at 77 K for PILC reference materials.

TABLE 4. Standard Isotherm Data for Nitrogen Adsorption at 77 K on Al-, Si-, Zr- and Fe-PILC$_{1273K}$ Materials

	Al-PILC$_{1273K}$	Si-PILC$_{1273K}$	Zr-PILC$_{1273K}$	Fe-PILC$_{1273K}$		Al-PILC$_{1273K}$	Si-PILC$_{1273K}$	Zr-PILC$_{1273K}$	Fe-PILC$_{1273K}$
p/p^0	α_s				p/p^0	α_s			
0.0001	0.019	0.008	0.062	0.075	0.1	0.339	0.316	0.527	0.563
0.0002	0.026	0.014	0.083	0.099	0.12	0.385	0.365	0.561	0.594
0.0003	0.031	0.016	0.096	0.114	0.14	0.430	0.416	0.595	0.624
0.0004	0.035	0.018	0.106	0.126	0.16	0.472	0.463	0.628	0.654
0.0005	0.038	0.020	0.115	0.136	0.18	0.515	0.509	0.661	0.683
0.0006	0.040	0.022	0.122	0.144	0.2	0.558	0.553	0.692	0.711
0.0007	0.043	0.023	0.128	0.152	0.225	0.611	0.615	0.732	0.745
0.0008	0.045	0.024	0.134	0.158	0.25	0.665	0.671	0.771	0.780
0.0009	0.047	0.026	0.139	0.164	0.275	0.720	0.732	0.812	0.816
0.001	0.049	0.027	0.144	0.170	0.3	0.775	0.789	0.852	0.852
0.0012	0.052	0.029	0.152	0.179	0.325	0.830	0.843	0.887	0.888
0.0014	0.055	0.031	0.160	0.188	0.35	0.886	0.894	0.926	0.923
0.0016	0.058	0.032	0.167	0.196	0.375	0.942	0.947	0.962	0.961
0.0018	0.060	0.033	0.173	0.203	0.4	1.000	1.000	1.000	1.000
0.0021	0.064	0.035	0.181	0.212	0.425	1.059	1.055	1.038	1.041
0.0024	0.067	0.037	0.188	0.220	0.45	1.120	1.111	1.079	1.084
0.0027	0.069	0.039	0.195	0.228	0.475	1.183	1.169	1.122	1.127
0.003	0.072	0.040	0.201	0.235	0.5	1.245	1.224	1.162	1.171
0.0034	0.075	0.043	0.208	0.244	0.525	1.306	1.276	1.207	1.217
0.0038	0.079	0.045	0.215	0.252	0.55	1.367	1.330	1.250	1.263
0.0043	0.083	0.047	0.223	0.261	0.575	1.430	1.392	1.296	1.312
0.0048	0.086	0.050	0.231	0.269	0.6	1.496	1.446	1.339	1.364
0.0053	0.090	0.052	0.237	0.277	0.625	1.568	1.512	1.391	1.424
0.0058	0.093	0.054	0.243	0.284	0.65	1.647	1.570	1.447	1.492
0.0063	0.096	0.057	0.249	0.290	0.675	1.722	1.629	1.503	1.566
0.0071	0.101	0.060	0.257	0.300	0.7	1.794	1.689	1.555	1.643
0.0076	0.103	0.062	0.262	0.305	0.725	1.877	1.752	1.613	1.728
0.0084	0.108	0.066	0.269	0.313	0.75	1.964	1.820	1.685	1.829
0.0092	0.112	0.069	0.276	0.321	0.775	2.052	1.892	1.769	1.968
0.01	0.116	0.072	0.282	0.327	0.8	2.136	1.963	1.867	2.110
0.0125	0.127	0.081	0.299	0.345	0.82	2.207	2.027	1.955	2.253
0.015	0.136	0.089	0.315	0.359	0.84	2.307	2.104	2.071	2.423
0.0175	0.144	0.096	0.327	0.372	0.86	2.418	2.185	2.230	2.664
0.02	0.151	0.104	0.338	0.383	0.88	2.545	2.283	2.434	2.925
0.025	0.165	0.118	0.356	0.401	0.9	2.706	2.378	2.741	3.298
0.03	0.179	0.133	0.373	0.417	0.91	2.807	2.443	2.954	3.494
0.035	0.192	0.147	0.387	0.432	0.92	2.925	2.515	3.207	3.719
0.04	0.204	0.160	0.401	0.445	0.93	3.064	2.602	3.532	4.010
0.05	0.228	0.188	0.425	0.469	0.94	3.223	2.718	3.975	4.314
0.06	0.252	0.215	0.448	0.490	0.95	3.420	2.887	4.590	4.703
0.07	0.275	0.240	0.470	0.510	0.96	3.655	3.057	5.435	5.121
0.08	0.296	0.265	0.489	0.528	0.97	3.975	3.365	6.631	5.690
0.09	0.318	0.291	0.508	0.545					

Al-PILC$_{1273K}$: S_{BET} = 2.42 m^2/g, $V^{0.4}$ = 0.72 cm^3 STP/g; Si-PILC$_{1273K}$: S_{BET} = 2.19 m^2/g, $V^{0.4}$ = 0.65 cm^3 STP/g; Zr-PILC$_{1273K}$: S_{BET} = 4.29 m^2/g, $V^{0.4}$ = 1.48 cm^3 STP/g; Fe-PILC$_{1273K}$: S_{BET} = 5.69 m^2/g, $V^{0.4}$ = 2.04 cm^3 STP/g

calcined at 1073 K and Fransil-I (Bhambhani *et al*. 1972) were included in this figure. Specific surface areas of the PILC reference materials were calculated at relative pressure ranges between 0.14 and 0.3. These S_{BET} values and the adsorbed volume at $p/p^0 = 0.4$ ($V^{0.4}$) are shown in Table 4, where the standard isotherms data are given.

As can be observed in Figure 6, the isotherms of the reference materials present significant differences among them at low and high relative pressures, suggesting the influence of the chemical nature of each material. Differences observed in the isotherms of non-porous reference materials for PILC could be due to the type of oxides that constitute the pillars. In addition, these materials present variations with respect to the NC_{1073K}, perhaps because it was calcined at a lower temperature than the PILC reference materials. By contrast, similar behaviour at low pressures is observed between Si-$PILC_{1273K}$ and Al-$PILC_{1273K}$ and between Fe-$PILC_{1273K}$ and Zr-$PILC_{1273K}$, which could be due to similarities in their surface chemical character. It can be observed that Fransil-I isotherm present differences with the PILC reference materials, perhaps due to the fact that the former is a hydroxylated siliceous material and the latter ones are aluminosilicates containing other oxides as well.

Table 5 shows textural properties of the PILCs studied, in which the micropore volumes were determined from the fits shown in Figure 7. The $V_{\mu P\text{-}DR}$ values were determined in a relative pressure range between 10^{-4} and 10^{-2}. The HJ equation was used in the t-plot method to evaluate $V_{\mu P\text{-}t}$. The α_s-plot method was applied using the respective standard isotherm of each PILC material. The $V_{\mu P\text{-}DFT}$ was obtained using the kernel for PILC surface with cylindrical pore geometry (Olivier and Occelli 2001) available in Micromeritics equipment software.

TABLE 5. Textural Properties of PILC Materials

Samples	S_{BET} (m^2/g)	$V_{\mu P\text{-}DR}$ (cm^3/g)	t-Plot		α_s-Plot		$V_{\mu P\text{-}DFT}$ (cm^3/g)
			$V_{\mu P\text{-}t}$ (cm^3/g)	S_{ext} (m^2/g)	$V_{\mu P\text{-}\alpha}$ (cm^3/g)	S_{ext} (m^2/g)	
Al-PILC	320	0.14	0.11	45	0.12	30	0.12
Si-PILC	520	0.20	0.12	250	0.19	160	0.15
Zr-PILC	210	0.10	0.06	55	0.07	45	0.07
Fe-PILC	230	0.09	0.02	180	0.04	150	0.06

From Figure 7 it can be seen that the DR plots of Al-, Zr- and Fe-PILC present deviations from linearity [Figures 7(e, g and h)], which could be related to the heterogeneity in their micropores (Gil *et al*. 2008). These deviations introduce some uncertainty in the calculation of micropore volumes. In addition, an overestimation of $V_{\mu P\text{-}DR}$ with respect to those obtained by the α_s-plot and the other methods can be seen as well. This overestimation increases in samples with a higher amount of mesopores than micropores (Zr- and Fe-PILC).

Otherwise, the $V_{\mu P\text{-}t}$ values were lower than those obtained by the α_s-plot and DFT methods, as shown in Figures 7(a-d). This underestimation could be related to the use of a t-equation (based on the adsorption data of non-porous Al_2O_3; de Boer *et al*. 1966), which has a different chemical nature than the PILC materials. In addition, a high dispersion in the micropore volumes obtained from the three different methods was observed in Si- and Fe-PILC samples, perhaps due to a lack in the definition of point B (the definition of point B is presented in Rouquerol *et al*. 1999) in their adsorption isotherms, as can be seen in Figure 5. This lack of definition also affects the selection of a reliable linear region for applying the t- and α_s-plot methods, as it was mentioned in other publications (Bhambhani *et al*. 1972).

An aspect worth mentioning here is that the kernel used in the application of the DFT method

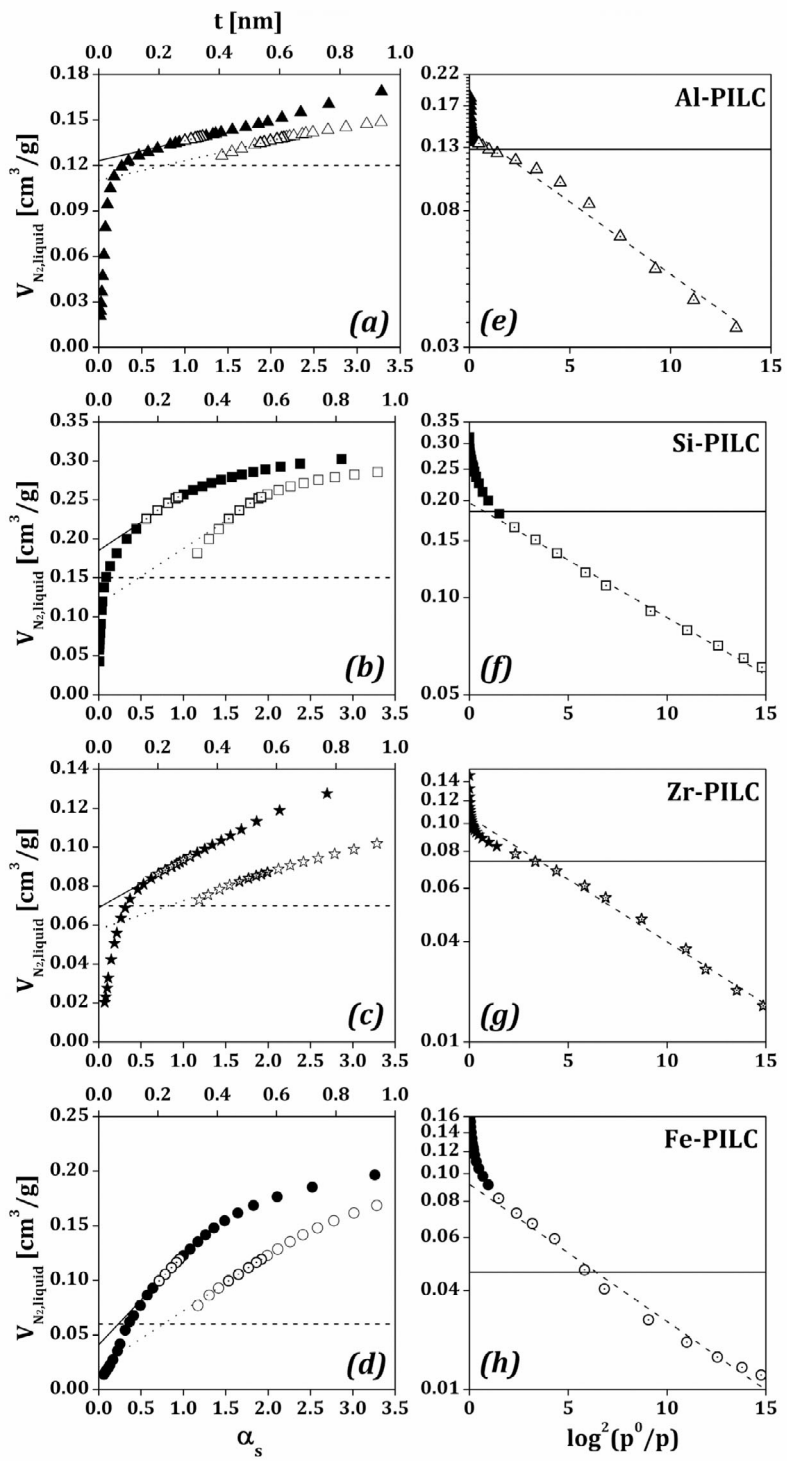

Figure 7. (a–d) t (open symbols) and α_s (filled symbols) plots and (e–h) DR plots with their respective fits for Al-, Si-, Zr- and Fe-PILC samples. Y axis intercepts correspond to $V_{\mu P\text{-}\alpha}$ (—), $V_{\mu P\text{-}t}$ (···) in (a), (b), (c) and (d); and $V_{\mu P\text{-}DR}$ (-·-) in (e), (f), (g) and (h). The horizontal dashed line in (a), (b), (c) and (d) represents the $V_{\mu P\text{-}DFT}$ value, while the horizontal solid line in (e), (f), (g) and (h) represents the $V_{\mu P\text{-}\alpha}$ value.

is the unique one available for PILC, and it considers pores with cylindrical geometry. However, it is known that the pores in the PILC correspond to slit-pore geometry (Gil and Montes 1994). Taking this fact into account, reliable micropore volumes were obtained by applying the α_s-plot method with standard isotherms for each PILC material to ensure that the reference material presents the same chemical nature. Anyway, the values of $V_{\mu P\text{-}\alpha}$ and $V_{\mu P\text{-}DFT}$ are in agreement with those observed in the characterization of the other porous materials under study.

CONCLUSIONS

In this work, a comparative study for the determination of micropore and mesopore volumes by different methods was carried out using several nanoporous materials. It was observed that for those samples that present a high proportion of mesoporosity, the micropore volume obtained by the DR equation is overestimated with respect to the other evaluated methods. This behaviour is independent of the pore geometry or the chemical nature of the samples.

By contrast, the other three analyzed methods showed similar micropore volumes. Nevertheless, the t-plot method showed small differences compared with the other methods, which could be due to its dependence on the chemical nature of the samples studied. These deviations are related to the use of empirical t equations that are not always accurate with the chemical nature of the material analyzed. Such equations could be avoided by using data from non-porous reference materials with similar chemical properties (α_s-plot method).

It was found that micropore volumes obtained by the α_s-plot method were in agreement with those obtained by the NLDFT and QSDFT methods in all the studied materials, despite the differences in their pore geometry and chemical nature. In the case of PILC materials, it was important to measure the high-resolution standard isotherms for each PILC, so as to ensure the validity of the reported results.

Therefore, based on the findings reported herein, it can be concluded that the α_s-plot method is a versatile and reliable method for characterizing nanoporous solids (achieved by selecting an appropriate standard isotherm) and obtaining the best results using high-resolution standard isotherms. Four high-resolution standard isotherms for Al-, Si-, Zr- and Fe-PILC materials were measured and reported in this work.

ACKNOWLEDGEMENTS

This work was financially supported by FONCYT, UNSL and CONICET (Argentina).

REFERENCES

Barrera, D., Villarroel-Rocha, J., Marenco, L., Oliva, M.I. and Sapag, K. (2011) *Adsorpt. Sci. Technol.* **29**, 975.

Bhambhani, M.R., Cutting, P.A., Sing, K.S.W. and Turk, D.H. (1972) *J. Colloid Interface Sci.* **38**, 109.

Broekhoff, J.C.P. and de Boer, J.H. (1967) *J. Catal.* **9**, 15.

Brouwer, S., Groen, J.C. and Peffer, L.A.A. (2007) The impact of mesoporosity on microporosity assessment by CO_2 adsorption, revisited. In: *Characterization of Porous Solids VII, Studies in Surface Science and Catalysis*, Vol. 160, P.L. Llewellyn, F. Rodriguez-Reinoso, J. Rouquerol and N. Seaton, editors. Elsevier, Amsterdam, p. 145.

Brunauer, S., Emmett, P.H and Teller, E. (1938) *J. Am. Chem. Soc.* **60**, 309.

Carabineiro, S.A.C., Thavorn-Amornsri, T., Pereira, M.F.R. and Figueiredo, J.L. (2011) *Water Res.* **45**, 4583.
Carrott, P.J.M., Roberts, R.A. and Sing, K.S.W. (1987) *Carbon* **25**, 769.
Corma, A. and García, H. (2002) *Chem. Rev.* **102**, 3837.
de Boer, J.H., Lippens, B.C., Linsen, B.G., Broekhoff, J.C.P., van den Heuvel, A. and Osinga, Th.J. (1966) *J. Colloid Interface Sci.* **21**, 405.
de Souza Santos, P. (1989) *Ciência e Tecnologia de Argilas*, Vol. 1. Edgard Blücher Ltda., São Paulo, Brazil.
Dubinin, M.M. (1960) *Chem. Rev.* **60**, 235.
Falabella, S. Aguiar, E., Liebsch, A., Chaves, B.C. and Costa, A.F. (1998) *Microporous Mesoporous Mater.* **25**, 185.
Farfan-Torres, E.M., Dedeycker, O. and Grange, P. (1991) Zirconium pillared clays. Influence of basic polymerization of the precursor on their structure and stability. In: *Preparation of Catalysts V, Scientific Bases for the Preparation of Heterogeneous Catalysts, Studies in Surface Science and Catalysis*, Vol. 63, G. Poncelet, P.A. Jacobs, P. Grange, B. Delmon, editors. Elsevier, Amsterdam, p. 337.
García Blanco, A.A., Amaya, M.G., Roca Jalil, M.E., Nazzarro, M., Oliva, M.I. and Sapag, K. (2011) *Top. Catal.* **54**, 190.
García Blanco, A.A., de Oliveira, J.C.A., López, R., Moreno-Piraján, J.C., Giraldo, L., Zgrablich, G. and Sapag, K. (2010) *Colloids Surf., A* **357**, 74.
Gil, A., Assis, F.C.C., Albeniz, S. and Korili, S.A. (2011) *Chem. Eng. J.* **168**, 1032.
Gil, A., Korili, S.A. and Vicente, M.A. (2008) *Catal. Rev. Sci. Eng.* **50**, 153.
Gil, A. and Montes, M. (1994) *Langmuir* **10**, 291.
Gor, G.Y., Thommes, M., Cychosz, K.A. and Neimark, A.V. (2012) *Carbon* **50**, 1583.
Gregg, S.J. and Sing, K.S.W. (1982) *Adsorption, Surface Area and Porosity*, 2nd Ed, Academic Press, New York.
Guan, C., Su, F., Zhao, X.S. and Wang, K. (2008) *Sep. Purif. Technol.* **64**, 124.
Halsey, G. (1948) *J. Chem. Phys.* **16**, 931.
Han, Y.-S., Matsumoto, H. and Yamanaka, S. (1997) *Chem. Mater.* **9**, 2013.
Harkins, W.D. and Jura, G. (1944) *J. Am. Chem. Soc.* **66**, 1366.
Ignat, M., Van Oers, C.J., Vernimmen, J., Mertens, M., Potgieter-Vermaak, S., Meynen, V., Popovici, E. and Cool, P. (2010) *Carbon* **48**, 1609.
Jaroniec, M., Kruk, M. and Olivier, J.P. (1999) *Langmuir* **15**, 5410.
Jun, S., Joo, S.H., Ryoo, R., Kruk, M., Jaroniec, M., Liu, Z., Ohsuna, T. and Terasaki, O. (2000) *J. Am. Chem. Soc.* **122**, 10712.
Kaneko, K., Ishii, C., Ruike, M. and Kuwabara, H. (1992) *Carbon* **30**, 1075.
Kockrick, E., Schrage, C., Borchardt, L., Klein, N., Rose, M., Senkovska, I. and Kaskel, S. (2010) *Carbon* **48**, 1707.
Kruk, M., Jaroniec, M. and Gadkaree, K.P. (1997a) *J. Colloid Interface Sci.* **192**, 250.
Kruk, M., Jaroniec, M. and Sayari, A. (1997b) *Langmuir* **13**, 6267.
Langmuir, I. (1916) *Phys. Rev.* **8**, 149.
Lippens, B.C. and de Boer, J.H. (1965) *J. Catal.* **4**, 319.
Lu, G.Q. and Zhao, X.S. (2004). Nanoporous materials: an overview. In: *Nanoporous Materials, Science and Engineering*, Vol. 4, G.Q. Lu, X.S. Zhao, editors. Imperial College Press, London, p. 1.
Magee, R.W. (1995) *Rubber Chem. Technol.* **68**, 590.
Nakai, K., Yoshida, M., Sonoda, J., Nakada, Y., Hakuman, M. and Naono, H. (2010) *J. Colloid Interface Sci.* **351**, 507.
Neimark, A.V., Lin, Y., Ravikovitch, P.I and Thommes, M. (2009) *Carbon* **47**, 1617.
Neimark, A.V. and Ravikovitch, P.I. (2001) *Microporous Mesoporous Mater.* **44–45**, 697.
Oliveira, L.C.A., Lago, R.M., Fabris, J.D. and Sapag, K. (2008) *Appl. Clay Sci.* **39**, 218.
Olivier, J.P. and Occelli, M.L. (2001) *J. Phys. Chem. B* **105**, 623.
Ravikovitch, P.I. and Neimark, A.V. (2006) *Langmuir* **22**, 11171.
Remy, M.J. and Poncelet, G. (1995) *J. Phys. Chem.* **99**, 773.

Roca Jalil, M.E., Vieira, R.S., Azevedo, D., Baschini, M. and Sapag, K. (2013) *Appl. Clay Sci.* **71**, 55.
Rodriguez-Reinoso, F., Martin-Martinez, J.M., Prado-Burguete, C. and McEnaney, B. (1987) *J. Phys. Chem.* **91**, 515.
Rouquerol, F., Rouquerol, J. and Sing, K.S.W. (1999) *Adsorption by Powders and Porous Solids: Principles, Methodology and Applications*, Academic Press, San Diego.
Sapag, K. and Mendioroz, S. (2001) *Colloids Surf., A* **187–188**, 141.
Seaton, N.A., Walton, J.P.R.B. and Quirke, N. (1989) *Carbon* **27**, 853.
Silvestre-Albero, A., Jardim, E.O., Bruijn, E., Meynen, V., Cool, P., Sepúlveda-Escribano, A., Silvestre-Albero, J. and Rodríguez-Reinoso, F. (2009) *Langmuir* **25**, 939.
Sing, K.S.W. (1968) *Chem. Ind.* **44**, 1520.
Sing, K.S.W. (1998) *Adv. Colloid Interface Sci.* **76–77**, 3.
Sing, K.S.W., Everett, D.H., Haul, R.A.W., Moscou, L., Pierotti, R.A., Rouquerol, J. and Siemieniewska, T. (1985) *Pure Appl. Chem.* **57**, 603.
Soares Maia, D.A., Sapag, K., Toso, J.P., López, R.H., Azevedo, D.C.S., Cavalcante Jr., C.L. and Zgrablich, G. (2010) *Microporous Mesoporous Mater.* **134**, 181.
Solar, C., García Blanco, A.A., Vallone, A. and Sapag, K. (2010). Adsorption of methane in porous materials as the basis for the storage of natural gas. In: *Natural Gas*, P. Potocnik, editor. Sciyo, Rijeka, Croatia, p. 205.
Srinivasu, P., Vinu, A., Hishita, S., Sasaki, T., Ariga, K. and Mori, T. (2008) *Microporous Mesoporous Mater.* **108**, 340.
Thommes, M. (2010) *Chem. Ing. Tech.* **82**, 1059.
Wang, S. (2009) *Microporous Mesoporous Mater.* **117**, 1.
Yamanaka, S., Doi, T., Sako, S. and Hattori, M. (1984) *Mater. Res. Bull.* **19**, 161.
Zhou, H., Zhu, S., Hibino, M., Honma, I. and Ichihara, M. (2003) *Adv. Mater.* **15**, 2107.